

7

Steady flow in open channels

7.1 Introduction

The flow of water in open channels is characterised by the existence of a 'free' surface i.e. an upper boundary in contact with air at atmospheric pressure. Gravity is the motive force. The term 'steady' implies that the velocity vector at a particular location does not change with time. We can distinguish three categories of steady flow in open channels:

- (1) uniform flow
- (2) gradually varied flow
- (3) rapidly varied flow

As defined in Chapter 2, steady uniform flow exists when the velocity vector is constant with respect to both time and space variables. In steady varied flow the magnitude of the velocity varies along the flow path. This variation may be gradual, for example, upstream of a flow-measuring device or rapid such as in a spillway discharge.

7.2 Hydraulic resistance to flow

The fundamental nature of the hydraulic resistance to flow in open channels is the same as that outlined in Chapter 3 for pipes flowing full. The flow Reynolds number for open channels is defined in terms of the channel hydraulic radius R_h :

$$R_e = \frac{vR_h\rho}{\mu} \tag{7.1}$$

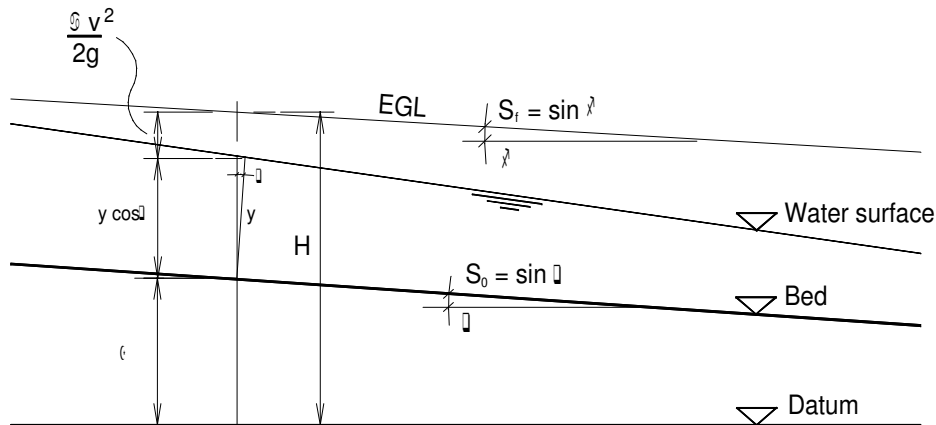


Fig 7.1 Components of total head H

When Reynolds number exceeds about 1100, as is invariably the case for water flow in open channels, the flow is turbulent. The flow energy parameters are defined in Fig 7.1:

$$H = z + y \cos \theta + \alpha \frac{v^2}{2g} \quad (7.2)$$

where H is the total head relative to an horizontal datum. The term specific head or specific energy E_s is also an important parameter in open channel flow. It is defined as

$$E_s = y \cos \theta + \alpha \frac{v^2}{2g} \quad (7.3)$$

that is, it is the total head relative to the channel bed as datum.

The EGL or friction slope S_f reflects the hydraulic resistance to flow. The expressions relating friction slope to pipe flow, presented in Chapter 3, can be adapted to open channel flow geometry by replacing the pipe diameter D by the channel hydraulic radius R_h , using the relationship $D = 4 R_h$.

Using this relationship, the open channel form of the Darcy-Weisbach equation becomes:

$$S_f = \frac{fv^2}{8gR_h} \quad (7.4)$$

where the friction factor f is given by the appropriately adapted form of the Colebrook-White equation (3.25):

$$\frac{1}{\sqrt{f}} = -0.88 \ln \left[\frac{k}{14.8R_h} + \frac{0.625}{R_e \sqrt{f}} \right] \quad (7.5)$$

Equations (7.4) and (7.5) may be combined to give the following explicit expression for velocity:

$$v = -\sqrt{6.2gR_h S_f} \ln \left[\frac{k}{14.8R_h} + \frac{0.625}{R_e \sqrt{f}} \right] \quad (7.6)$$

Where flow is in the rough turbulent category, as in most natural channels, equation (7.6) may be simplified by the omission of the Reynolds number term, giving

$$v = 7.8\sqrt{R_h S_f} \ln \left[\frac{14.8R_h}{k} \right] \quad (7.7)$$

As already noted in Chapter 3, the Manning equation was developed for open channel flow computation. Its generally used form is

$$v = \frac{1}{n} R_h^{0.67} S_f^{0.5} \quad (3.32)$$

The following correlation of Manning's n and equivalent sand roughness k is derived from equations (7.7) and (3.32):

$$\frac{1}{n} = 7.8R_h^{-0.167} \ln \left[\frac{14.8R_h}{k} \right] \quad (7.8)$$

which may be simplified to the following form

$$\frac{1}{n} = \frac{C_n}{k^{0.167}} \quad (7.9)$$

where C_n is a function of the ratio R_h/k , as defined by equations (7.8) and (7.9), resulting in the following numerical value range:

R_h/k	10	100	1000	10 000
C_n	26.48	26.39	23.63	19.94

(note that k is in m in the foregoing correlations with the Manning n -value).

Recommended surface roughness values for use in design are given in Table 7.1 (refer also to Table 3.1 for additional surface roughness data relating to pipes).

Table 7.1
Recommended values for the surface roughness parameter k
(Hydraulics Research 1990)

	k-value (mm)		
	Good	Normal	Poor
Slimed sewers*			
(a) Half-full velocity about 0.75 ms ⁻¹			
Concrete, spun or vertically cast	-	3.0	6.0
Asbestos-cement	-	3.0	6.0
Clayware	-	1.5	3.0
uPVC	-	0.6	1.5
(b) Half-full velocity about 1.2 ms ⁻¹			
Concrete, spun or vertically cast	-	1.5	3.0
Asbestos-cement	-	0.6	1.5
Clayware	-	0.3	0.6
uPVC	-	0.15	0.3
Unlined rock tunnels			
Granite and other homogeneous rocks	60	150	300
Diagonally bedded slates	-	300	600
Earth channels			
Straight uniform artificial channels	15	60	150
Straight natural channels, free from shoals, boulders and weeds	150	300	600

*The roughness of a slimed sewer varies considerably during any year. The normal value is that roughness which is exceeded for approximately half the time. The poor value is that which is exceeded, generally on a continuous basis, for one month of the year. The value of k should be interpolated for velocities between 0.75 and 1.2 ms⁻¹.

7.2.1 Influence of channel shape on flow resistance

The most commonly used channel cross-sections are rectangular, trapezoidal and circular. Expressions for the section flow parameters for these sections are given on Fig 7.2.

The hydraulic resistance to flow in an open channel of a given cross-sectional area is minimised by minimising its wetted perimeter length. For a rectangular section of given cross-sectional area A , the channel proportions, which minimise the perimeter length P are found as follows:

$$P = B + 2y = \frac{A}{y} + 2y$$

$$\frac{dP}{dy} = -\frac{A}{y^2} + 2 = 0 \quad \text{for } P_{\min}$$

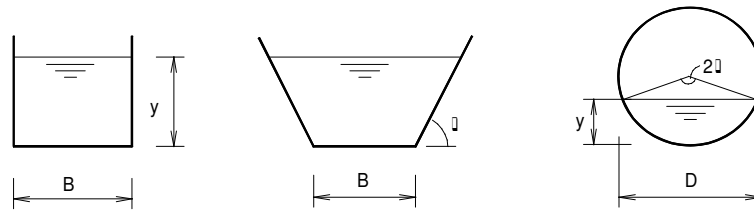


Fig 7.2 Section parameters

	Rectangular	Trapezoidal	Circular
A	By	$Y(B + y/\tan \theta)$	$\frac{D^2}{4}(\theta - 0.5\sin 2\theta)$
R_h	$\frac{By}{B + 2y}$	$\frac{y(B + y / \tan \theta)}{B + 2y / \sin \theta}$	$\frac{D}{4} \left(\frac{\theta - 0.5\sin 2\theta}{\theta} \right)$

Hence at P_{\min} , $B = 2y$, that is, the most efficient shape of rectangular section from a discharge viewpoint is one in which the flow depth is half the width. It may also be noted that an inscribed semicircle can be fitted to this section profile.

In a trapezoidal section of given area A, the wetted perimeter length can be expressed as a function of the flow depth y and the angle of inclination, θ , of the sidewall to the horizontal:

$$P = B + \frac{2y}{\sin \theta} = \frac{A}{y} - \frac{y}{\tan \theta} + \frac{2y}{\sin \theta}$$

The values of y and θ , which minimise P for a given value of A, are found from the relationships:

$$\frac{dP}{dy} = \frac{\partial P}{\partial y} + \frac{\partial P}{\partial \theta} \frac{d\theta}{dy} = 0$$

$$\frac{dP}{d\theta} = \frac{\partial P}{\partial \theta} + \frac{\partial P}{\partial y} \frac{dy}{d\theta} = 0$$

which simplify to the following conditions:

$$\frac{\partial P}{\partial y} = 0 \quad (7.10)$$

$$\frac{\partial P}{\partial \theta} = 0 \quad (7.11)$$

Differentiation of P with respect to y in accordance with eqn (7.10) results in the relationship:

$$B + \frac{2y}{\tan \theta} = \frac{2y}{\sin \theta} \quad (7.12)$$

Differentiation of P with respect to θ in accordance with (7.11) results in the relationship:

$$\cos \theta = 0.5 \quad (7.13)$$

Equation (7.12) infers a surface width equal to twice the sidewall length, while eqn (7.12) indicates a 60° sidewall inclination to the horizontal. These requirements are satisfied by an equilateral trapezoidal section, which can be circumscribed by a semi-circle having the surface width as diameter.

Circular section conduits (pipes) are widely used in open channel flow mode, particularly in sewerage systems. The variations with depth of flow of the flow parameters of principal interest are shown on Fig 7.3. It is of design interest to note that velocity at half depth is the same as the flowing-full value. The theoretical maximum discharge occurs at a flow depth ratio y/D equal to 0.87. Attention is drawn to the computational instabilities, which may be encountered at flow depths in the vicinity of the maximum flow depth ratio. For practical design purposes it is recommended that the flowing-full value be used as the effective maximum discharge capacity for circular section conduits used as open channels.

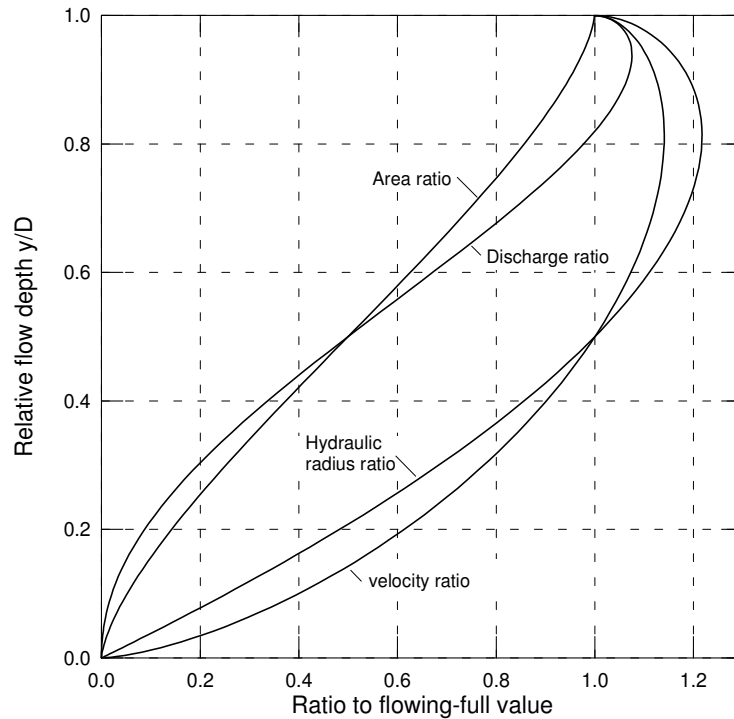


Fig 7.3 Flow in part-full circular pipes.

$$\frac{R_h}{R_{h0}} = \left(1 - \frac{\sin 2\theta}{2}\right) \quad \frac{v}{v_0} = \left(1 - \frac{\sin 2\theta}{2}\right)^{2/3}$$

$$\frac{A}{A_0} = \frac{1}{\pi} \left(1 - \frac{\sin 2\theta}{2}\right) \quad \frac{Q}{Q_0} = \left(1 - \frac{\sin 2\theta}{2}\right)^{2/3} \left(\theta - \frac{\sin 2\theta}{2}\right) \frac{1}{\pi}$$

7.3 Computation of uniform flow

The Manning and Darcy-Weisbach equations for open channel flow incorporate the three flow variables, velocity v , friction slope S_f and hydraulic radius R_h . Thus, given any two of these variables the third may be computed. In many

cases, designers may prefer to replace the variable v and R by the related variables, discharge Q and flow depth y , respectively.

Assembling the known terms on the right-hand side:

$$\text{Manning:} \quad Q = \frac{A}{n} R_h^{0.67} S_f^{0.5} \quad (7.14)$$

$$A^{1.5} R_h = (nQ)^{1.5} S_f^{-0.75} \quad (7.15)$$

$$S_f = \left(\frac{nQ}{A} \right)^2 R_h^{-1.33} \quad (7.16)$$

$$\text{Darcy-Weisbach:} \quad Q = A \left(\frac{8gR_h S_f}{f} \right)^{0.5} \quad (7.17)$$

$$A^2 R_h = \frac{fQ^2}{8gS_f} \quad (7.18)$$

$$S_f = \frac{f}{8gR_h} \left(\frac{Q}{A} \right)^2 \quad (7.19)$$

The parameters A and R_h are functions of the flow depth y .

7.3.1 ARTS software

The ARTS software includes an open channel object in its tool palette, which can be assigned any of the foregoing cross-sectional shapes. The program calculates the steady flow depth and mean velocity for specified values of channel gradient and wall roughness, based on the Darcy-Weisbach equations.

7.4 Specific energy

Specific energy E_s is defined as the total head relative to the channel bed:

$$E_s = y \cos \theta + \alpha \frac{v^2}{2g} \quad (7.20)$$

when $\cos \theta$ is taken as unity and v is replaced by Q/A , we get:

$$E_s = y + \frac{\alpha Q^2}{2gA^2} \quad (7.21)$$

For a given discharge Q , the value of the flow depth y and, hence E_s , changes as the channel slope is changed. The flow depth at which E_s has a minimum value is known as the critical depth y_c . Its value is found by differentiating E_s with respect to y :

$$\frac{dE_s}{dy} = 1 - \frac{\alpha Q^2}{gA^3} \left(\frac{dA}{dy} \right)$$

For minimum E_s , $dE_s/dy = 0$, hence

$$\frac{\alpha Q^2}{gA^3} \left(\frac{dA}{dy} \right) = 1 \quad (7.22)$$

Since $dA = W dy$, where W is the channel width at the water surface, eqn (7.22) may be written in the form

$$\frac{\alpha W Q^2}{gA^3} = 1 \quad (7.23)$$

Equation (7.23) defines the condition of minimum specific energy and hence the critical depth y_c .

For a rectangular section and taking $\alpha = 1$, equation (7.23) simplifies to

$$\frac{v^2}{gy_c} = 1 \quad (7.24)$$

The ratio v / \sqrt{gy} is known as the Froude number Fr . It is essentially a measure of the ratio of inertial to gravitational forces in the flow regime. When the depth of flow exceeds y_c ($Fr < 1$), the flow is described as subcritical or tranquil; when the depth of flow is less than y_c ($Fr > 1$), the flow is described as supercritical. The variation of E_s as a function of flow depth for a rectangular channel is plotted on Fig 7.4.

An important attribute of critical flow is that it defines a unique relationship between mean velocity and flow depth and hence the creation of critical flow provides the basis of many open channel flow measurement structures.

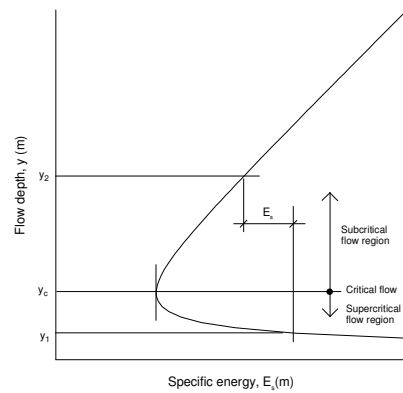


Fig 7.4 Energy-defined flow regimes

7.5 Rapidly varied steady flow: the hydraulic jump

It is clear from Fig 7.4 that for a given specific energy value, two flow depths are feasible, one subcritical and the other supercritical. A smooth transition from supercritical to subcritical flow is not feasible (unconfined deceleration); instead we get a hydraulic jump, as illustrated on Fig 7.5.

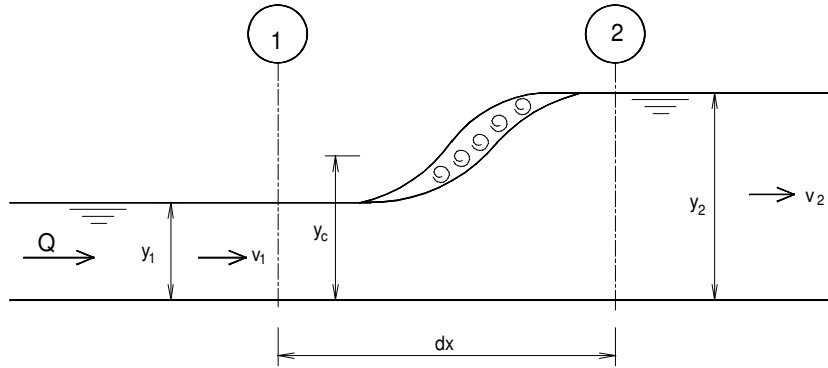


Fig 7.5 Hydraulic jump

The relation between the incident and sequent depth in an hydraulic jump is found by applying the momentum principle to the control volume between sections 1 and 2:

$$\rho g A_1 \bar{y}_1 - \rho g A_2 \bar{y}_2 + \rho g \bar{A} dx S_0 - \rho g \bar{A} dx S_f = \rho Q (v_2 - v_1) \quad (7.25)$$

where \bar{y}_1 and \bar{y}_2 represent the depth of the centroid at sections 1 and 2, respectively and \bar{A} is the mean of A_1 and A_2 . Neglecting the weight and friction terms, this simplifies to

$$A_1 \bar{y}_1 - A_2 \bar{y}_2 - \frac{Q}{g} (v_2 - v_1) = 0 \quad (7.26)$$

Applied to a rectangular channel of width B:

$$y_1^2 - y_2^2 - \frac{2Q}{Bg} (v_2 - v_1) = 0$$

which simplifies to

$$y_1^2 y_2 + y_1 y_2^2 - \frac{2q^2}{g} = 0 \quad (7.27)$$

where $q = Q/B$ is the discharge per unit width.

Solving for the sequent depth y_2 :

$$y_2 = -\frac{y_1}{2} + \left(\frac{y_1^2}{4} + \frac{2q^2}{gy_1} \right)^{0.5} \quad (7.28)$$

or expressed in terms of the Froude number:

$$y_2 = \frac{y_1}{2} \left\{ \left(1 + 8F_{r1}^2 \right)^{0.5} - 1 \right\} \quad (7.29)$$

where $F_{r1} = v_1 / \sqrt{gy_1}$. Similarly, equation (7.27) may be solved to find the incident depth y_1 , when the sequent depth y_2 is known:

$$y_1 = \frac{y_2}{2} \left\{ \left(1 + 8F_{r2}^2 \right)^{0.5} - 1 \right\} \quad (7.30)$$

The character of the hydraulic jump can be qualitatively classified by its incident Froude number value (Chow, 1959), with best performance in the F_{r1} value range 4.5 to 9.0. In this range the channel length over which the jump takes place is about six times the downstream depth.

There is a loss of energy in the hydraulic jump, as illustrated on Fig 7.4. This loss E_L is

$$E_L = E_1 - E_2 = \left(y_1 + \frac{v_1^2}{2g} \right) - \left(y_2 + \frac{v_2^2}{2g} \right) \quad (7.31)$$

which simplifies to:

$$E_L = \frac{(y_2 - y_1)^3}{4y_1y_2} \quad (7.32)$$

7.5 Gradually varied flow

In gradually varied steady open channel flow, velocity and depth vary along the channel length but are invariant with time at any particular location. Such flow occurs in the vicinity of control sections, in channel transitions where there is a change of channel slope or cross-section, in collector channels, as used in sedimentation tanks and sand filters, and in channels with side overflow weirs, as used for storm overflow purposes. Some typical gradually varied water surface profiles are illustrated on Fig 7.6. Referring to Fig 7.1, the total head H , as expressed by equation (7.2), may be written in the form

$$H = Z + y \cos \theta + \frac{\alpha Q^2}{2gA^2} \quad (7.33)$$

differentiating with respect to x :

$$\frac{dH}{dx} = \frac{dZ}{dx} + \frac{dy}{dx} \cos \theta + \alpha \left(\frac{q}{gA^2} \frac{dQ}{dx} - \frac{Q^2}{gA^3} \frac{dA}{dx} \right) \quad (7.34)$$

The term dA/dx can be expressed as the product

$$\frac{dA}{dy} \frac{dy}{dx} = W \frac{dy}{dx}$$

where W is the channel width at water surface level. Assuming $\cos \theta$ equal to unity, eqn (7.34) can be written as

$$-S_f = -S_0 + \frac{\alpha Q}{gA^2} \frac{dQ}{dx} + \frac{dy}{dx} \left(1 - \frac{aWQ^2}{gA^3} \right)$$

which results in the following expression for the water surface slope dy/dx :

$$\frac{dy}{dx} = \frac{S_0 - S_f - \frac{\alpha Q}{gA^2} \frac{dQ}{dx}}{1 - \alpha \frac{WQ^2}{gA^3}} \quad (7.35)$$

Where the lateral inflow/outflow is zero ($dQ/dx = 0$), the foregoing expression becomes

$$\frac{dy}{dx} = \frac{S_0 - S_f}{1 - \frac{\alpha W Q^2}{g A^3}} \quad (7.36)$$

The water surface in gradually varied flow is found by integration of equation (7.35) or (7.36), as appropriate, subject to the particular prevailing upstream and/or downstream boundary values for the flow depth y .

7.6 Computation of gradually varied flow

Equation (7.35) or (7.36) can be numerically integrated using fourth order Runge-Kutta numerical computational scheme (Chapra and Canale, 1985) in which the flow depth change ($y_{i+1} - y_i$), over a channel length Δx , is calculated as follows:

$$y_{i+1} = y_i + \frac{\Delta x}{6} (k_1 + 2k_2 + 2k_3 + k_4) \quad (7.37)$$

where

$$k_1 = f(x_i, y_i), \quad k_2 = f(x_i + 0.5\Delta x, y_i + 0.5\Delta x k_1)$$

$$k_3 = f(x_i + 0.5\Delta x, y_i + 0.5\Delta x k_2), \quad k_4 = f(x_i + \Delta x, y_i + \Delta x k_3)$$

In this case $f(y) = dy/dx$, as given by (7.35) or (7.36)

The k -terms may be regarded as measures of $\ddot{A}\ddot{A}$ within the channel interval Δx under consideration,

$\frac{1}{6}(k_1 + 2k_2 + 2k_3 + k_4)$ being the estimate of its mean value. The cumulative discretization error associated with the fourth order Runge-Kutta method is proportional to Δx^4 . Computational accuracy is thus greatly increased by reducing the channel step length Δx . In this regard, it should be noted that the surface water slope changes rapidly when the flow depth is close to the critical depth and hence, to achieve accuracy in this region, Δx should be assigned a small value. Computation starts from a control section at which the flow depth y is known. Proceeding along the channel in steps of Δx , successive flow depths are calculated using equation (7.33). The channel reach in which gradually varied flow prevails may be upstream or downstream of the control section. It should be noted that Δx is positive in the downstream direction and negative in the upstream direction.

7.6.1 Computation of water surface profile using ARTS software

The ARTS software package (Aquavarra Research, 2000) facilitates computation of the water surface profile from a specified starting depth using a fourth order Runge-Kutta numerical integration scheme. It caters for rectangular, trapezoidal and circular section channels and for the following three categories of gradually varied flow:

- (1) computation of water surface profiles in channels without lateral inflow.
- (2) computation of water surface profiles in collector channels with a uniform lateral inflow rate.
- (3) computation of water surface profile and overflow discharge in channels with side weirs.

Figs 7.6a and 7.6b illustrate water surface profiles, typical of gradually varied flow belonging in flow category (1). The water surface slope for this category is defined by equation (7.36). The program user must input a starting flow depth, which may be at a downstream control, as in Fig 7.6a, or at an upstream control, as in Fig 7.6b. In addition to computing the flow depth at specified Δx intervals in the channel reach of interest, the program also computes the normal and critical depths for the given discharge, as these frequently represent boundary or limiting values for the computation. The program outputs the flow depth at channel intervals corresponding to the selected computational step length Δx .

Fig 7.6c illustrates a gradually varied flow profile characteristic of flow category (2), that is, flow in a collector/decanting channel of the type widely used in water processing units such as sand filters and sedimentation tanks. The illustrated channel has a uniform lateral inflow over its length and a free overfall at its outlet end. Equation (7.35) defines the water surface slope for this category of gradually varied flow. The program user must specify the total lateral inflow rate, which is assumed to be uniformly distributed over the channel length. Computation starts from the outlet end where the flow depth is assumed to be critical depth. As a practical means of avoiding the computational difficulties associated with the critical depth, referred to above, the program uses a value of $1.02 y_c$ as its starting depth at the outlet end of the channel. The program outputs the flow depth at intervals equal to the computational step Δx along the channel, starting from the discharge end.

Fig 7.6d illustrates a gradually varied flow profile characteristic of flow category (3), that is, flow in a channel reach in which there is a lateral discharge over side overflow weirs. The water surface slope for this flow type is described by equation (7.35). In this instance the lateral discharge $q_L = -dQ/dx$ is not constant but varies with the weir head H_w in accordance with the weir equation:

$$q_L = C_w H_w^{1.5} \quad (7.38)$$

where C_w is a variable weir coefficient. Program GVF uses the following empirical expression for the weir coefficient C_w , based on experimental results reported by Frazer (1957):

$$C_w = 2.29 - \frac{y_c}{y} - \frac{0.08y_c}{L_w} \quad (7.39)$$

where L_w is the side weir length. The computational scheme used in program GVF assumes constant overflow discharge over the computational step length Δx , based on the value of the weir head H_w at the upstream end of the Δx reach. The program outputs the overflow weir head, the overflow discharge, the channel flow depth and the channel discharge rate, for each computational step, over the side weir length.

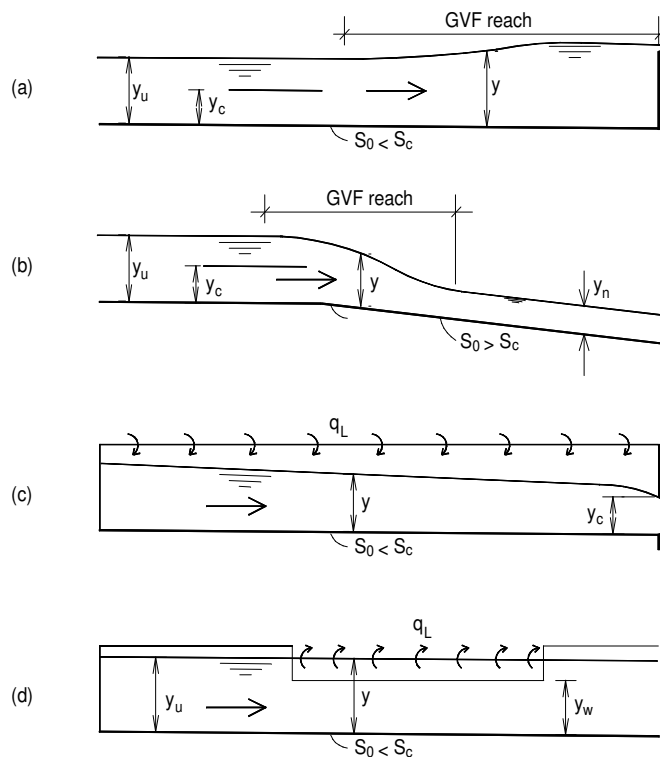


Fig 7.6 Typical gradually varied flow examples ($S_0 =$ bottom slope, $S_c =$ critical slope)
 (a) GVF profile in channel of subcritical slope; (b) GVF profile due to bed slope change;
 (c) GVF profile in collector channel; (d) GVF profile in channel with side weir overflow.

7.8 Channel transitions

A channel transition is typically a short length of channel over which there is a change in cross-section and/or slope and hence a change in velocity under steady flow conditions. Transitions are used to connect channels of different sizes and are often associated with flow-measurement structures.

Where the flow regime throughout a transition channel is entirely subcritical or entirely supercritical, equations (7.35) or (7.36), as appropriate, may be used to compute the variation in flow depth. In expanding or contracting channels the channel width W at water surface level may be expressed as a function of the flow depth y and space variable x .

Where the flow regime changes from subcritical to supercritical within a transition section, passing through critical depth in the process, the transition acts as a 'control section', that is, a section which effectively controls the flow depth. This type of transition forms the basis of many open channel flow measurement structures, as discussed in Chapter 8.

Where the flow changes from supercritical to subcritical in a transition via a hydraulic jump, the location of the latter may be determined using the computational procedures outlined in Section 7.5.

Abrupt changes in channel cross-section give rise to local energy losses which are analogous to the form losses associated with pipe fittings. The energy loss ΔH due to an abrupt expansion may be shown from momentum considerations to be

$$\Delta H = \frac{(v_u - v_D)^2}{2g} \quad (7.40)$$

where v_U and v_D are the mean upstream and downstream velocities, respectively. The head loss can be reduced to about one-third of this value by using a side wall taper of 1:4 in the channel expansion (Henderson 1966).

The energy losses associated with channel contractions are less than those for channel expansions. They are conveniently expressed in terms of the downstream velocity head:

$$\Delta H = K \frac{v_D^2}{2g}$$

where K has a value of about 0.23 for sharp-edged contractions in rectangular channels and about 0.11 when the edges are rounded.

7.8.1 Entry flow to closed conduits

The transition from open to closed conduit flow is a frequently encountered flow regime in water engineering practice. It merits particular attention because entry conditions may sometimes exert a controlling influence on the discharge capacity of the closed conduit.

Where the closed conduit entry is fully submerged and flowing full throughout its length, the computation of its steady discharge rate is straightforward, being a function of the difference between the upstream and downstream water levels and the integrated hydraulic resistance of the closed conduit.

Where the conduit entry is partly submerged or operating at a low submergence, entry conditions may effectively control the discharge rate if the immediate closed conduit has a supercritical slope, as illustrated on Fig 7.7. Under these circumstances the flow passes through critical depth at the conduit entrance, which acts as a control section. This condition may prevail even when the conduit entrance is submerged, being maintained by air entrainment due to vortex formation associated with flow acceleration towards the entrance. The transition from open channel to fully closed conduit flow is brought about by a hydraulic jump at some distance downstream of the entrance, as shown on Fig 7.7.

In general, the entrainment of air at closed conduit entrances is undesirable and may significantly reduce the discharge capacity. Where flow acceleration is unavoidable at closed conduit entrances, air intake at low submergence levels can be prevented by the use of anti-vortex baffles (Blaisdell, 1960).

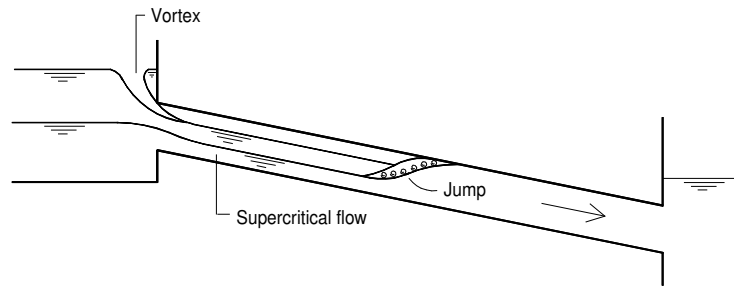


Fig 7.7 Flow profiles at the entrance to a closed conduit of steep slope at the inlet end

References

- Blaisdell, F. W. (1960) Hood inlet for closed conduit spillways. Proc. ASCE, 86, No. HY5, p.7.
- Chapra, S. C. and Canale, R. P. (1985) Numerical Methods for Engineers, McGraw-Hill Book Company, New York.
- Chow, V. T. (1959). Open-channel Hydraulics, McGraw Hill Book Co., Inc., New York.
- Frazer, W. (1957) The behaviour of side weirs in prismatic rectangular channels, Proc. Inst. Civ. Engrs, London, 6, p305-327.
- Henderson, F. M. (1966) Open Channel Flow, The Macmillan Co., New York.
- Hydraulics Research, Wallingford (1990) Charts for the hydraulic design of channels and pipes, 6th. ed., Thomas Telford Ltd., London.